Magnetic ordering of $TbMn_2D_2$ - a nuclear magnetic resonance analysis

2001 J. Phys.: Condens. Matter 13 6115

(http://iopscience.iop.org/0953-8984/13/27/305)

INSTITUTE OF PHYSICS PUBLISHING JOURNAL OF PHYSICS: CONDENSED MATTER

J. Phys.: Condens. Matter **13** (2001) 6115–6121 PII: S0953-8984(01)23159-2

Magnetic ordering of $TbMn_2D_2$—a nuclear magnetic resonance analysis

S Leyer[1], G Fischer[1], E Dormann[1,3], A Budziak[2] and H Figiel[2]

[1] Physikalisches Institut, Universität Karlsruhe (TH), D-76128 Karlsruhe, Germany
[2] Department of Solid State Physics, Faculty of Physics and Nuclear Techniques, University of Mining and Metallurgy, Al. Mickiewicza 30, 30-059 Cracow, Poland

E-mail: edo@piobelix.physik.uni-karlsruhe.de (E Dormann)

Received 2 March 2001, in final form 8 May 2001
Published 22 June 2001
Online at stacks.iop.org/JPhysCM/13/6115

Abstract

Nuclear magnetic resonance of ^{2}D nuclei is measured in the paramagnetic phase of $TbMn_2D_2$ powder samples. Static and dynamic contributions of Mn and Tb moments to the nuclear probes are characterized on approach to the ordering temperature $T_N = 272$ K and the possibility of antiferromagnetic correlations between Mn and Tb magnetic moments is analysed. Field and temperature dependence of the magnetization in the ordered state is presented as well.

1. Introduction

The magnetic ordering temperature of cubic Laves phase compounds RMn_2H_x increases by more than 30% with hydrogen charging for $1.5 < x < 3.5$ and R = Y, Dy, Tb, Gd [1–4]. Recently, we showed that the accompanying lattice expansion—and especially the increased Mn–Mn separation—changes also the quasi-critical behaviour reflected by μSR and ^{1}H/^{2}D nuclear spin-relaxation on approach to the antiferromagnetic ordering temperature of $YMn_2(H/D)_x$ [5, 6]. In this respect the nuclei on the tetrahedral interstitial sites with two R and two Mn nearest neighbours are convenient probes for the spin fluctuations and antiferromagnetic correlations on the Mn and R sublattices. Increased hydrogen content and Mn–Mn spacing increases not only the ordering temperature T_N, but modifies also the wave-vector dependence of exchange interaction or dynamic susceptibility [5, 6]. Structural distortions and ordered H/D superstructures are additional problems of these hydrides, however, that have to be considered for a complete magnetostructural phase diagram.

On the other hand, we have established by a comprehensive experimental and theoretical analysis of the magnetism of RMn_6Ge_6 intermetallic compounds, that their high-temperature magnetic ordering is due to the manganese sublattices [7–9]. The rare earth moments are primarily polarized via 3d–5d wave function extension and hybridization, followed by

[3] Corresponding author.

ferromagnetic Hund's rule rare earth 5d–4f exchange [9]. The R–R exchange interaction of RKKY type [10] and crystal field effects are at the origin of the frequently observed complicated magnetic structures at low temperature, but R–R exchange interaction without R–Mn coupling would generate R sublattice magnetic ordering at substantially lower temperatures than the Mn-sublattice ordering, only [7, 9]. For the RMn_6Ge_6 ternary intermetallic compounds, the Mn–R exchange interaction is comparatively weak and the coupling constant falls only in the 1–10 K range [9], polarizing the R sublattice ferrimagnetically already above its own ordering temperature.

Thus it is interesting to compare the spin dynamics of RMn_2D_2 ($R \neq Y$) with the results for YMn_2D_x, using the ^2D nuclear spin resonance and relaxation as the local probe on approach to the antiferromagnetic (or ferrimagnetic) ordering temperature close to room temperature. We show below, that the ^2D ($I = 1$) nucleus reflects in $TbMn_2D_2$ only the manganese sublattice spin fluctuations in its quasi-critical behaviour close to $T_N = 272$ K.

2. Experimental details and results

The sample was prepared from high purity starting elements using the standard induction melting technique, and then annealed, to obtain a well defined single phase material. X-ray analysis was used for phase control before and after hydriding, which was achieved by applying usual technologies [3].

Magnetic properties of a powder sample were measured with a SQUID magnetometer (Quantum Design MPMS) with the sample surrounded by helium atmosphere during the measurements. Data were recorded at fixed field strength for increasing temperature (increasing the field strength after cooling). Magnetic moment data are shown in figure 1. In order to know the magnetic behaviour of $TbMn_2D_2$ appropriate for the ^2D-NMR analysis in the paramagnetic state, the independence of the susceptibility M_ρ/H on the field strength was verified. This is visualized by the data points and solid line in the upper part of figure 2. For comparison, as solid line, a Curie–Weiss fit

$$\chi = \frac{C}{T - \theta_p} + \chi_{dia} \tag{1}$$

is included with $\chi_{dia} = -1.6 \times 10^{-7}$ cm^3 g^{-1} from tabulated data [11]. A ferromagnetic Weiss temperature $\theta_p = +8.1(\pm 1.7)$ K is derived, and an effective paramagnetic moment per formula unit

$$\mu_{eff} = \sqrt{C_{mol} \cdot 3k_B N_{mol}^{-1}} = (9.01 \pm 0.03)\,\mu_B. \tag{2}$$

Nuclear magnetic resonance was measured for the same sample in the paramagnetic phase at varied temperature for fixed magnetic field (70 kOe) using a Bruker MSL 300 spectrometer. Due to the non-spherical shape of the powder grains and the cylindrical shape of the sample tube, the demagnetizing field causes a relatively large half width at half height $\Delta\nu_{1/2}$ and a non-negligible part of the ^2D-NMR line peak position's shift $\delta\nu$ (plotted with respect to a perdeuterotoluene (PDT) standard in figure 2 and 3) [12, 13]. The solid line shown in the $\Delta\nu_{1/2}$ data in the middle part of figure 2 proves the proportionality of the width to the magnetic susceptibility (upper part and equation (1)), as must be expected for predominating demagnetization broadening. In contrast to the magnetic susceptibility of $TbMn_2D_2$ being much larger than that of YMn_2D_2, the variation of $\delta\nu$ with T is much smaller than in the latter system analysed earlier [6]. It is important to note that the ^2D-NMR line of $TbMn_2D_2$ shifts towards positive values $\delta\nu$ on approach of the ordering temperature, that is contrary to the observation for YMn_2D_2.

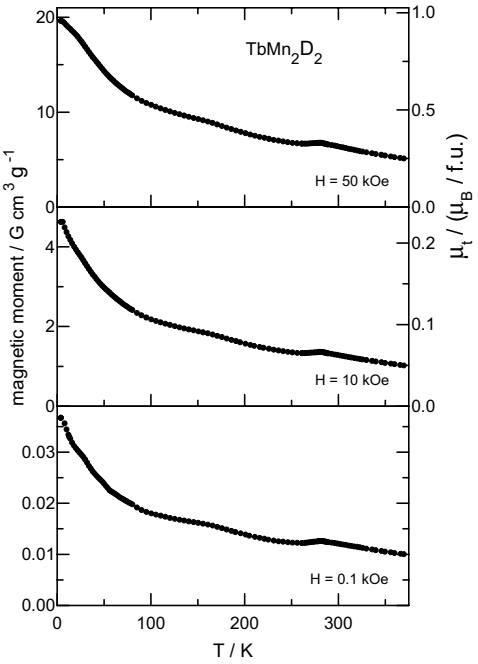

Figure 1. Temperature dependence of the weight related magnetic moment of a $TbMn_2D_2$ powder sample for 3 different field strength values H = 50 kOe, 10 kOe and 0.1 kOe, measured for increasing temperature. The high-field data are also converted into total moment per formula unit μ_t, see right hand scale.

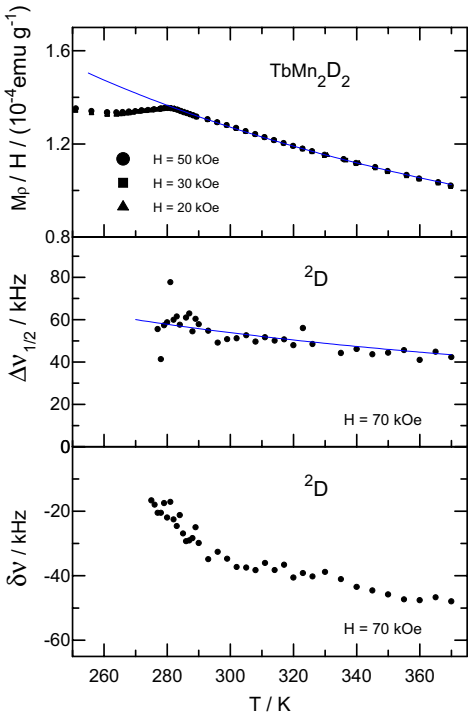

Figure 2. Temperature dependence of static magnetic properties of $TbMn_2D_2$ in the paramagnetic range: Magnetic susceptibility per gram M_ρ/H (upper part). ^{2}D-NMR characteristics at H = 70 kOe: half-width at half height, $\Delta\nu_{1/2}$ (middle), and peak position relative to perdeuterotoluene (PDT) standard $\delta\nu$ (lower part). Solid lines are explained in text.

Longitudinal (T_1) and transversal (T_2) relaxation of the ^{2}D nuclei was derived using three-pulse stimulated echo or two-pulse echo decay, respectively [14]. Phase cycling, quadrature detection, signal accumulation and integration of the fourier transform of the second half of the echo were adopted as usual [6]. Figure 4 shows relaxation rates ($1/T_1$ and $1/T_2$) obtained for the paramagnetic phase of the $TbMn_2D_2$ powder sample.

3. Discussion

The low-field magnetization data, shown on an enlarged scale in the lower part of figure 1, give the proof for the adequate quality of the $TbMn_2D_2$ sample used for the current NMR analysis. Pure Tb, that might be accumulated in the grain boundaries of $TbMn_2$ due to a small Tb excess in the starting composition, would give dramatic low-field contributions below its ferromagnetic ordering around 220–230 K. If deuterated to the dideuteride TbD_2, it would produce weak antiferromagnetic ordering anomalies around 18 K (T_N of TbH_2, [15]) or below the temperature range studied in the case of TbD_3. $TbMn_2$ should be identified by its canted antiferromagnetic ordering below 54 K [16, 17]. Because all of these signatures are, at most, weakly present, the current sample seems to be superior in quality than the standard 5% impurity limit that x-ray analysis could detect.

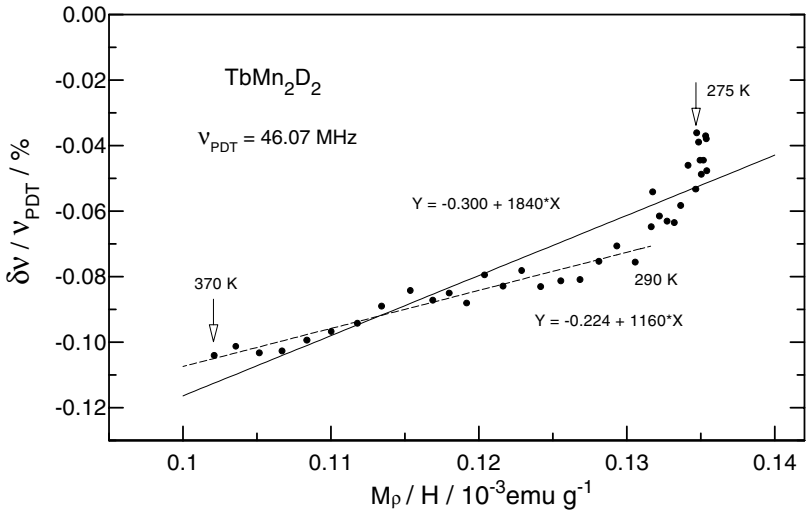

Figure 3. Relation between ^{2}D line shift $\delta\nu/\nu_{PDT}$ and susceptibility M_ρ/H for $TbMn_2D_2$. For the solid or broken line fit, all data or the data for $T \geqslant 290$ K, only, were taken into account. Fit equation is given in the figure.

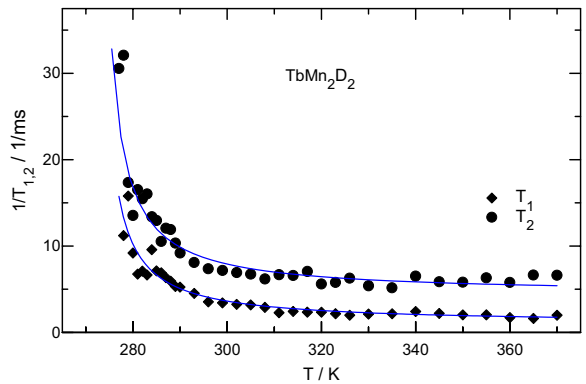

Figure 4. Temperature dependence of ^{2}D longitudinal and transversal relaxation rates $1/T_1$ and $1/T_2$ of $TbMn_2D_2$ in the paramagnetic phase (46.05 MHz). The solid line fits are explained in the text.

The antiferromagnetic ordering around 280 K is clearly discernable for all field strengths, see figures 1 and 2, but the value of T_N would have a relatively large error bar, if it were based on the magnetic analysis of this powder sample alone. Fortunately, ^{2}D-NMR relaxation reflects the Néel temperature rather critically, yielding T_N = (272.0 ± 1.5) K for the current sample (see below). Thus this sample of $TbMn_2D_2$ orders at higher temperature than YMn_2H_2 (T_N = 243 K, [5]), but lower than $GdMn_2H_2$ (T_N = 308.1 K, [2]) and $TbMn_2H_2$ ($T_N = 284 \pm 6$) K). The integral magnetic moment of our powder sample does not allow the decision, if the weak magnetic anomaly close to 180 K reflects a magnetic reorientation transition [18] or not. Even for this powder sample, our highest field strength of 50 kOe remains insufficient to orient the Tb^{3+} moment of $(g \cdot J =)9\mu_B$ plus the Mn moments parallel to the field direction at low temperature, as can be visualized from the right hand scale of figure 1. The weak reduction of the total moment at T_N points to the fact that, primarily, the manganese moments

order antiferromagnetically and the Tb-sublattices are merely polarized by external and af-manganese exchange fields instead of spontaneously ordered just below T_N. Thus we assume that the exchange coupling strength decreases in the sequence: Mn–Mn, Mn–Tb, and Tb–Tb. Similar conclusions were reported for $TbMn_2D_{4.5}$ [18]. The antiferromagnetic ordering of the Mn sublattices as well as of the ordered components of the Tb sublattices for $TbMn_2D_2$ was derived from a recent neutron diffraction investigation at 1.5 K, 100 K, and 200 K [19]. Additional polarizable components of the Tb^{3+} moments were deduced even for the magnetic structure at 1.5 K.

We will now focus on the paramagnetic range. The Curie–Weiss fit shown as a solid line in the upper curve of figure 2 yields an effective moment of $\mu_{\text{eff}} = (9.01 \pm 0.03)\mu_B$ per formula unit to be compared with a high temperature limiting value $\mu_{\text{eff}} = 9.72\mu_B$ for Tb^{3+} and typically 2.7–4μ_B for manganese, alone. Because the difference between $(9.72\mu_B)^2$ and $(9.01\mu_B)^2$ amounts just to 13.37 $\mu_B^2 \approx 2(2.59\mu_B)^2$, it is tempting to speculate that in the 80 K range close above T_N, Tb^{3+} and Mn moments are ferrimagnetically correlated, already. This assumption is supported by the temperature dependence of the ^{2}D-NMR line shift reported in the lower part of figure 2.

We have shown that the relative ^{2}D-NMR line shift

$$\delta\nu(T)/\nu_0 = K_0 + \alpha \cdot \chi_{\text{mol}}(T)/N_A \tag{3}$$

of YMn_2D_x can be described with values of the slope or coupling constant α amounting to $-(2.0 \pm 1.0)$ kOe μ_B^{-1} for $1.5 \leqslant x \leqslant 2.5$ [6]. For $YMn_2D_{2.5}$ the slope α changes from a larger negative value of $\alpha = -3.0$ kOe μ_B^{-1} at higher temperatures, to a slope of only -1.0 kOe μ_B^{-1} close to T_N.

Figure 3 shows the $\delta\nu(T)$ data of figure 2 plotted as a function of the magnetic susceptibility with the temperature as an implicit parameter. The slope presented by the solid line (taking all data into account) amounts to $\alpha = +0.38$ kOe μ_B^{-1} (with $K_0 = -0.3\%$), i.e. by a factor of five smaller and, most remarkably, with opposite sign compared to YMn_2D_x. If the fit is restricted to the high temperature range $T \geqslant 290$ K, a smaller slope of $\alpha = +0.24$ kOe μ_B^{-1} (and $K_0 = -0.224\%$) is obtained (broken line). Thus, in $TbMn_2D_2$, like in $YMn_2D_{2.5}$, the coupling constant α tends to more positive values on approach to the ordering temperature, being negative for YMn_2D_x but positive for $TbMn_2D_2$. A negative slope would be expected from demagnetization, already: according to the shape of our sample (tube), $(N - 4\pi/3)$ can be estimated at 0.82 (or 6.5% of 4π), resulting in a demagnetizing field slope of $\alpha_N = -0.12$ or -0.07 kOe/μ_B, depending on whether x-ray or effective powder density is taken into account. Thus the range $\alpha_T = +0.31 \ldots 0.50$ kOe μ_B^{-1} is estimated for the transferred contribution via conduction electrons or classical dipolar fields of spin and orbital moments in $TbMn_2D_2$. Neutron diffraction on $TbMn_2D_2$ at $T = 320$ K show that the deuterium atoms are shifted away from the centre of the 2Mn–2Tb tetrahedra to positions (0.42, 0.42, 0.14) [19]. At this site the two Mn neighbours are at equal distance, but the two Tb neighbours at different, and closer, separation. The comparably small positive value of α_T points to a partial compensation of the Tb^{3+} and Mn static transferred contributions. We will now consider the dynamics of these contributions.

As can be seen from figure 4, the ^{2}D relaxation rates increase dramatically upon approach to the antiferromagnetic ordering temperature T_N. The solid lines show the best fit of the quasi-critical behaviour with the relation

$$\frac{1}{T_{1,2}} = R_{1,2}\left(\frac{T - T_N}{T_N}\right)^{-\eta} + \left(\frac{1}{T_{1,2}}\right)_0. \tag{4}$$

We refer to reference [5, 6] for an explanation of the interactions and model assumptions justifying this description.

On approach to the Néel temperature, the slowing down of the relevant spin fluctuations yields the first term with $\eta = 1/2$ according to the model of Moriya [20]. It was shown recently, that μSR and NMR relaxation in YMn_2D_x can be parametrized even in a more extended temperature range with this relation, if the adjustment of the parameter η is allowed for [5,6]. A roughly linear increase of η with x was observed, i.e. from $\eta \approx 0.35$ for $x = 0$ to $\eta = 1.2$ for $x = 3.0$, with $\eta \approx 0.88 \pm 0.05$ for YMn_2D_2. It was argued that η reflects the wave-vector dependence of the exchange interaction or dynamic susceptibility [5]. For $TbMn_2D_2$, the ^{2}D nuclei have two Tb ions in addition to the two Mn atoms as nearest neighbours, thus they are subject to static and dynamic contributions of rare earth and manganese moments. Because the weakness of the susceptibility anomaly at T_N indicates that primarily the manganese sublattices order at T_N, whereas for the Tb sublattices the influence of external field and Tb–Mn exchange coupling compete, we introduced the additional constant term in equation (4) in order to describe the non-critical contribution of the Tb moments to the ^{2}D relaxation rates near T_N (of Mn). $T_N = 270.5$ K and 273.6 K was derived from the independent fit to the T_1 or T_2 data, respectively. The parameters derived from the longitudinal and transversal relaxation rate using the average value $T_N = 272$ K are compiled in table 1. Due to the added Tb-contribution, outside the critical range both rates are faster than in YMn_2D_x for $x \approx 2$ [6]. The similarity of the quasi-critical behaviour of $1/T_1$ and $1/T_2$ for YMn_2D_x and $TbMn_2D_2$ gives credit to our interpretation, that the manganese sublattices order antiferromagnetically at T_N.

Table 1. Parameters used for fit of ^{2}D relaxation rates in $TbMn_2D_2$, as explained in text.

	$R_{1,2}$	η	$(1/T_{1,2})_0$
$1/T_1$	$0.343\,ms^{-1}$	0.937	$0.99\,ms^{-1}$
$1/T_2$	$0.076\,ms^{-1}$	1.462	$4.54\,ms^{-1}$

It is interesting to discuss the value $\eta = 1.20 \pm 0.26$ obtained from this fit. It is larger than the value $\eta \approx 0.88 \pm 0.05$ derived for YMn_2D_2 at the same deuterium content. Thus spin fluctuations of YMn_2D_2 and $TbMn_2D_2$ differ, just as do their ordering temperatures $T_N = 243$ K and 272 K, respectively. Using the linear correlation between η and x of YMn_2D_x [5,6], we conclude that the spin fluctuations of $TbMn_2D_2$ close to T_N correspond to those of YMn_2D_x with $x > 2.2$, which, due to the smaller size of Y^{3+} compared to Tb^{3+}, has roughly the same value for T_N as $TbMn_2D_2$. This supports the argument for an antiferromagnetic ordering, driven primarily by the Mn sublattices of $RMn_2(H/D)_x$, taking place at T_N [18]. The value of the ordering temperature as well as the details of the dynamical susceptibility, which are reflected by the quasi-critical behaviour of nuclear spin-relaxation (i.e. q-dependence), are affected by the Mn–Mn separation. The size and not the moment of the R-neighbours seems to be of relevance.

4. Conclusions

$TbMn_2D_2$ orders antiferromagnetically at about $T_N = 272 \pm 1.5$ K. This report focusses on the paramagnetic phase, but the static magnetic properties of $TbMn_2D_2$ in the magnetically ordered state are presented as well. The ^{2}D nuclear spin-relaxation rates in the paramagnetic temperature range increase quasi-critically as $((T - T_N)/T_N)^{-\eta}$ with an exponent $\eta \approx 1.2$, comparable to the behaviour of YMn_2D_x for higher deuterium content, but similar ordering temperature. We conclude that the spin fluctuations of the manganese sublattice predominate at T_N. The Curie constant of the static magnetic susceptibility yields an effective moment of about 9 μ_B/f.u., thus smaller than the Tb^{3+} free ion contribution. Furthermore, the coupling constant

between electronic magnetization and hyperfine field at the ^{2}D nucleus, $\alpha_T \approx +0.4$ kOe μ_B^{-1}, is smaller by almost a factor of five and of opposite sign compared to YMn_2D_x. Both pieces of evidence point to antiferromagnetic correlations between Tb^{3+} and Mn moments already on approach to the af ordering temperature T_N.

Acknowledgments

We are grateful for financial support by the BMBF in the frame of the German–Polish scientific and technological cooperation between Karlsruhe and Krakow (project WTZ POL98/019) and by the Polish State Committee for Scientific Research (grant No 2 PO3B-144-15).

References

[1] Przewoznik J, Paul-Boncour V, Latroche M and Percheron-Guégan A 1996 *J. Alloys Compounds* **232** 107
[2] Przewoznik J, Zukrowski J and Krop K 1998 *J. Magn. Magn. Mater.* **187** 337
[3] Figiel H, Przewoznik J, Paul-Boncour V, Lindbaum A, Gratz E, Latroche M, Escorne M, Percheron-Guégon A and Mietniowski P 1998 *J. Alloys Compounds* **274** 29
[4] Przewoznik J, Zukrowski J, Freindl K, Japa E and Krop K 1999 *J. Alloys Compounds* **284** 31
[5] Paja A, Mietniowski P and Figiel H 2000 *Acata Phys. Pol. A* **97** 867
[6] Figiel H, Budziak A, Mietniowski P, Kelemen M T and Dormann E 2001 *Phys. Rev.* B **63** 104403
[7] Rösch P, Kelemen M T, Dormann E, Tomka G and Riedi P 2000 *J. Phys.: Condens. Matter* **12** 1065
[8] Kelemen M T, Rösch P, Kaplan N and Dormann E 2000 *Eur. J. Phys. B* **18** 435
[9] Kelemen M T, Brooks M S S and Dormann E 2001 *J. Phys.: Condens. Matter* **13** 657
[10] Yosida K 1996 *Theory of Magnetism* (Berlin: Springer)
[11] Sellwood P W 1956 *Magnetochemistry* (New York: Interscience) p 78
[12] Mozurkewich G, Ringermacher H I and Bolef D I 1979 *Phys. Rev.* B **20** 33
[13] Dormann E 1991 *NMR in intermetallic compounds Handbook on the Physics and Chemistry of Rare Earth* ed K A Gschneidner Jr and L Eyring (Amsterdam: North Holland) p 63
[14] Hahn E L 1950 *Phys. Rev.* **80** 580
[15] Daou J N, Vajda P and Burger J P 1988 *Phys. Rev.* B **37** 5236
[16] Nesbitt E A, Williams H J, Wernick J H and Sherwood R C 1963 *J. Appl. Phys.* **34** 1347
[17] Labroo S, Ali N, Robinson P 1990 *J. Appl. Phys.* **67** 5292
[18] Goncharenko I N, Mirebeau I, Irodova A V and Suard E 1999 *Phys. Rev.* B **59** 9324
[19] Budziak A, Figiel H, Zukrowski J, Gratz E and Ouladdiaf B to be published
[20] Moriya T 1962 *Progr. Theor. Phys.* **28** 371